

Magnetocapacitance, magnetoelasticity, and magnetopiezoelectric effect in $\text{HoFe}_3(\text{BO}_3)_4$

Cite as: Low Temp. Phys. **44**, 1341 (2018); <https://doi.org/10.1063/1.5078631>

Published Online: 31 December 2018

L. S. Kolodyazhnaya, G. A. Zvyagina, I. V. Bilych, K. P. Zhekov, N. G. Burma, V. D. Fil', and I. A. Gudim



[View Online](#)



[Export Citation](#)



[CrossMark](#)

ARTICLES YOU MAY BE INTERESTED IN

[Piezoelectric response in \$\text{SmFe}_3\(\text{BO}_3\)_4\$, a non-piezoactive configuration. The surface piezoelectric effect](#)

Low Temperature Physics **43**, 924 (2017); <https://doi.org/10.1063/1.5001291>

[Features of electronic paramagnetic resonance in the \$\text{ErAl}_3\(\text{BO}_3\)_4\$ single crystal](#)

Low Temperature Physics **44**, 863 (2018); <https://doi.org/10.1063/1.5049175>

[Is \$\text{LiCoPO}_4\$ a pyroelectric?](#)

Low Temperature Physics **43**, 1240 (2017); <https://doi.org/10.1063/1.5008421>

The advertisement features a blue background with a green optical cavity diagram. The text on the left reads: "LOW TEMPERATURE TECHNIQUES", "OPTICAL CAVITY PHYSICS", "MITIGATING THERMAL & VIBRATIONAL NOISE". At the bottom, a green button says "DOWNLOAD THE WHITE PAPER" and includes the URL "downloads.montanainstruments.com/optical_cavities". The Montana Instruments logo is on the right, with the tagline "COLD SCIENCE MADE SIMPLE".

Magnetocapacitance, magnetoelasticity, and magnetopiezoelectric effect in $\text{HoFe}_3(\text{BO}_3)_4$

L. S. Kolodyazhnaya,¹ G. A. Zvyagina,¹ I. V. Bilych,¹ K. P. Zhekova,¹ N. G. Burma,¹
V. D. Fil',^{1,a)} and I. A. Gudim²

¹*Verkin Institute for Low Temperature Physics and Engineering, National Academy of Sciences of Ukraine pr. Nauki, 47, Khar'kov, 61103, Ukraine*

²*Kirensky Institute of Physics, Siberian Branch, Russian Academy of Sciences Akademgorodok, 50, Krasnoyarsk, 660036, Russia*

(Submitted October 19, 2018)

Fiz. Nizk. Temp. **44**, 1712–1720 (December 2018)

The main components of the tensor of the moduli of elasticity and the piezomodulus have been measured in monocrystals of the ferroborate $\text{HoFe}_3(\text{BO}_3)_4$. The spin-dependent contributions to sound velocity, dielectric permeability, and piezoelectric response in the antiferromagnetic state were studied. The parameters of magnetoelectric and magnetoelastic interactions in an easy-plane magnetic-ordering phase have been defined. A phenomenological interpretation of observed effects is given. *Published by AIP Publishing.* <https://doi.org/10.1063/1.5078631>

Ferroborates (general formula $\text{RFe}_3(\text{BO}_3)_4$, where R is a rare earth or Y) are ordered in the antiferromagnetic phase at Néel temperatures (T_N) 30–40 K. The value of T_N is determined by the interaction in the ferric subsystem, and depends weakly on the type of REM (rare earth metal) ion. Magnetic measurements to very low temperatures do not detect intrinsic ordering in a rare earth subsystem that is polarized only due to *f-d* interaction. However, the type of REM ion substantially affects the position of the magnetic moments of iron relative to the crystallographic axes. In $\text{YFe}_3(\text{BO}_3)_4$, the spins of the iron are ordered in the base plane (easy-plane configuration). In the case of magnetic ions, both easy-axis (R = Dy, Tb, Rg), and easy-plane (R = Sm, Nd, Eu, Eg) configurations are realized.¹ In Ho and Gd ferroborates, the easy-plane phase that occurred below T_N is transformed at $T \sim 5\text{--}10$ K into easy-axis by means of spontaneous spin-reorientation transformation. In turn, the easy-axis phase can be transferred to easy-plane by imposing a magnetic field parallel to the easy axis (spin-flop).

All ferroborates crystallize in the non-centrally-symmetric trigonal phase of class 32 (D_3). Below T_N , in the absence of a magnetic field the equilibrium state is a polydomain structure; as a result some physical fields, such as spontaneous polarization in the base plane, are mutually compensated. The enantiomorphism inherent in this crystalline class leads to the same result.² And if in the first case the imposition of a single-domain magnetic field eliminates this compensation, it is impossible to prevent the contribution of enantiomorphism.

Interest in studying rare earth ferroborates is caused first of all by the significant magnetoelectric effects that occur in easy-plane phases. The reason for their occurrence is associated with the very small anisotropy in the base plane, due to which the significant magnitude of the “electric susceptibility of rotation”³ is manifested, i.e., the abnormally large effect of the electric field on the orientation of the vector of antiferromagnetism in the base plane. In Sm and Nd ferroborates, static measurements in the single-domain field detect the value of polarization to be $\sim 500 \mu\text{C/m}^2$.^{3,4} For the same reason, enormous values of magnetocapacitance ($\sim 100\%$)³ are observed also in these compounds.

A consequence of small basis anisotropy is likewise the significant magnitude of the “deformation susceptibility of

rotation”, the strong dependence of the orientation state of a spin system on its deformation. As a result, in the magnetic-ordering phase are observed both an enormous renormalization of the nonzero component of the tensor of the piezomodulus (the so-called magnetopiezoelectric effect),^{5,6} and the emergence of new tensor components that had been absent in the paraphase.⁷

All effects associated with the susceptibilities of rotation and with an increase in the magnetic field attenuate due to the increased rigidity of the magnetic subsystem. Nevertheless, studies of the magnetic-field dependences of magnetocapacitance and the magnetopiezoelectric effect make it possible, with the appropriate experimental geometry, to find the parameters that define the intensity of magnetoelectric and magnetoelastic interactions.^{5,6}

In addition to susceptibilities of rotation, other mechanisms are also possible, leading to the “entanglement” of the electric, magnetic and elastic subsystems of the magnetic-ordering environment. For example, the coefficients of magnetoelectric coupling may depend on the deformation, which results in renormalization of the piezoelectric response up to its emergence in a centrally-symmetric crystal. Such an effect has been observed in the LiCoPO_4 monocrystal.⁸ The marks of renormalization of the piezoelectric response are also found in neodymium ferroborate.⁶

This article is devoted to studying the magnetocapacitance, magnetoelasticity, and magnetopiezoelectric effect in $\text{HoFe}_3(\text{BO}_3)_4$. The motivation for this study results generally from the following circumstance. In the work⁹ devoted to this compound, it was observed that the dielectric permeability increases in the antiferromagnetic phase by a factor of almost two. At the same time, the measurement results of polarization presented in Ref. 9 detect an effect that does not exceed $100 \mu\text{C/m}^2$. This result is represented as rather strange, since both effects are controlled by the same parameter of magnetoelectric coupling, and the enormous value of magnetocapacitance would have to correspond to much larger values of polarization. In our opinion, the role was played in this case, apparently, by enantiomorphism.

In addition, as measurements have shown,¹⁰ compounds based on Sm and Nd turned out to be rather strong piezoelectric

materials, which can find practical application at usual room temperatures. For this reason, there is a certain interest also in the clarification of the value of the piezomodulus for holmium compounds, all the more as in this case there was also a theoretical estimate.¹¹

Experimental equipment

Monocrystals of $\text{HoFe}_3(\text{BO}_3)_4$ are grown by the method described in Ref. 12. The samples under study were cut from a monocrystal bulk and were oriented by means of radiography using the Laue method. Samples had a form close to a rectangular parallelepiped, with characteristic edge sizes ~ 2 mm. The sides of the samples were orthogonal to the main crystallographic directions. Accuracy of orientation was $\sim 1^\circ$.

All measurements were performed on equipment operating in pulsed mode and representing bridge or compensatory schemes, automatically balanced by amplitude and phase.¹³ The working frequencies were ~ 55 MHz. In order to separate the analyzed signals from adjustments due to the excitation pulse, as well as for time division of various acoustic modes, delay lines were used. In measuring absolute values of sound velocity, the use of delay lines is critically necessary.¹³ Delays are made from a monocrystal of Mo orientation [110]. The material of the delays is sufficiently polluted for suppression of electron attenuation in the helium region of temperatures.

The measurement procedure included:

- Measurements of both absolute sound velocities and of their relative changes. Absolute measurements included determination of the piezomodulus. Lithium-niobium piezoelectric transducers were used to generate acoustic signals. Silicon-organic GKZh-94 fluid was used as the acoustic binding.
- High-frequency measurements of the relative changes of dielectric permeability in the magnetic-ordering phase, depending on temperature and the magnitude and direction of the magnetic field. Here, the studied sample was located between the electrodes forming the capacitance of the differentiator circuit.
- Measurements of the relative changes of the piezomodulus in the antiferromagnetic state. In this case, the electric response arising in a sample due to its excitation by elastic deformation was recorded. More detailed description of the measurement procedure according to items 2 and 3 is provided in Ref. 5.

Moduli of elasticity and the piezomodulus

Measurements of the absolute values of sound velocities S are performed at liquid nitrogen temperature. Table 1 presents the results.

Here L , T , QL , and QT designate purely longitudinal, purely transverse, quasi-longitudinal and quasi-transverse modes, respectively. The vectors of displacements for $\mathbf{q} \parallel [010]$ in the QL and QT modes lie in the plane (100), and the vector of displacements in the T mode is orthogonal to this plane. Measurement precision is $\sim 0.3\%$. The chief contribution to this error is systematic error. Let us recall that the phase-frequency characteristics (PFC) of the studied sample in the procedure in Ref. 13 are obtained by the

TABLE 1. Velocity of sound (10^5 cm/s) in $\text{HoFe}_3(\text{BO}_3)_4$.

$\mathbf{q} \parallel$	[001]	[100]	[010]
Mode S	L 6.69	T 3.65	L 8.2 QL 8.14 QT 3.4 T 4.3

subtraction, from the PFC of a sandwich made of the sample and two delay lines, of the PFC of just the delay lines. However, in the formation of the diverse PFC, a “spare” layer of acoustic binding not compensated for by the subtraction procedure also participates. The thickness of this layer is $\sim 1.5\text{--}2$ μm , but since the sound velocity in the hardened cement is approximately three times slower, this leads to the specified systematic error.

An algorithm for finding the elastic modulus and the piezomodulus with reference to the specific symmetry of the studied crystals is described in Ref. 10. The x-ray value of density $\rho = 4.52$ g/cm and dielectric permeability $\epsilon = 20$ is used in the calculations.⁸ Table 2 shows the results by comparison with theoretical calculation.¹¹

The value of the piezomodulus $e_{11} \equiv e_{xxx}$ was defined from the ratio^{10,14}

$$\frac{4\pi e_{11}^2}{\epsilon \rho} = S_{L[100]}^2 - S_{QL[010]}^2 + S_{T[001]}^2 - S_{QT[010]}^2. \quad (1)$$

Clearly, there is no accumulation of systematic errors in calculation (1), and we estimate the accuracy of definition of e_{11} as approximately 10%.

The values obtained differ hardly at all from the corresponding values for the Sm and Nd ferroborates.¹⁰

Magnetocapacitance

Figure 1 illustrates the nature of the development of dielectric permeability ϵ_{xx} in various magnetic fields oriented in the base plane. Qualitatively these dependences are close to the results presented in Ref. 9. Below the Néel temperature the spin-dependent contribution to ϵ increases as the derivative increases, and at the point of spin reorientation ($T \sim 4.8$ K) the effect abruptly disappears. However, on the scale of changes these results are approximately 4 times less than those given in Ref. 9 – if in Ref. 9 for $H=0$ the increase is recorded at 100%, in our experiments the increase of ϵ in similar conditions did not exceed 25%. All results given below and their analysis pertain to the easy-plane phase.

As also in Sm⁵ and Nd⁶ ferroborates studied earlier, the form of these dependences is essentially defined by the orientation of \mathbf{H} in the xy plane. For $\mathbf{H} \parallel \mathbf{x}$ or $\mathbf{H} \parallel \mathbf{y}$, the effect is practically zeroed out upon reaching the field of single-domain value ($H \sim 0.5$ T).

At the same time, for $\mathbf{H} \parallel [110]$ the decrease in the effect extends to much greater fields.

TABLE 2. Moduli of elasticity (GPa) and piezomodulus (C/m^2) of $\text{HoFe}_3(\text{BO}_3)_4$.

Modulus	C_{11}	C_{33}	C_{44}	C_{12}	C_{14}	e_{11}
Our data	291.5	202.3	60.2	149.1	43.7	1.48
Calculated ¹¹	370	159	68	125	30	0.99

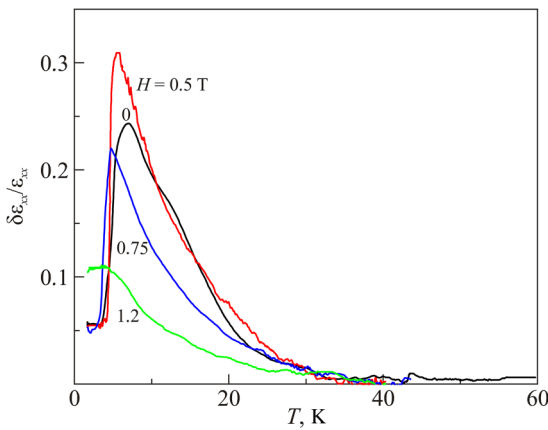


Fig. 1. Temperature dependences of relative changes of dielectric permeability for various values of the magnetic field $H \parallel [110]$.

The incomplete thermodynamic potential that permits analyzing the behavior of ϵ_{xx} can be presented in the following form Refs. 5 and 6 (Here and thereafter, only the part of thermodynamic potential that has relationship to the situation being studied is written. For example, in the case of magnetoelectric interaction the invariant term relative to symmetry operations is written as: $F_{ME} \sim E_x(l_x^2 - l_y^2) - 2E_yl_xl_y$. But since we are interested only in the part of the potential that is proportional to E_x , the term with E_y is dropped.)

$$\tilde{F} = -\frac{\epsilon_p E_x^2}{8\pi} + \frac{a_{Fe}}{2} E_x(l_x^2 - l_y^2) + \frac{a_{Ho}}{4} \sum_i E_x(\mu_x^{i2} - \mu_y^{i2}) + F_{in} - \frac{1}{2} \mathbf{M}\mathbf{H}. \quad (2)$$

Here ϵ_p is the dielectric permeability of the parphase. The two following members are the magnetoelectric contributions from the antiferromagnetic-ordering iron sublattice and the total contribution of the two rare-earth paramagnetic sublattices in the magnetic bias field H_{ex} of iron. F_{in} is the contribution to the potential of plane anisotropy and internal tensions of magnetoelastic origin. The last component is the Zeeman energy (\mathbf{M} is the total magnetic moment induced by an external field).

The decomposition in (2) is performed using the direct cosines of the vector of antiferromagnetism (l) and the magnetic moments of the holmium sublattices (μ^i). We recall that, since there is anti-translation in the magnetic symmetry group of ferroborates, a linear magnetoelectric effect in them is forbidden.

Due to the maximally large total moment of the Ho ion, the magnetic susceptibility of $\text{HoFe}_3(\text{BO}_3)_4$ is defined primarily by the rare earth. Magnetic measurements^{9,15} have shown that up to fields of ~ 2 T, the magnetic moment of $\text{HoFe}_3(\text{BO}_3)_4$ changes almost linearly with the magnetic field. Taking into account the anomalously small value of the magnetic bias field ($H_{ex} \sim 2.5$ T¹⁶), the magnetic moment of the holmium sublattices can be presented in the form $\mathbf{m}^i = \chi_{Ho} \mathbf{H}_{eff}^i = \chi_{Ho} ((-1)^i \mathbf{H}_{ex} + \mathbf{H})$. Here χ_{Ho} is the magnetic susceptibility of the REM in the sublattice, the index $i = 1, 2$ differentiates the ions of Ho that are located in the exchange field of different ferric sublattices, and the field \mathbf{H}_{ex} coincides in direction with the antiferromagnetism vector. In angular

variables φ and φ_H , representing the deviation from the x axis of the vectors \mathbf{H}_{ex} and \mathbf{H} , respectively, Eq. (2) is written as

$$\tilde{F} = -\frac{\epsilon_p E_x^2}{8\pi} + \frac{a_{Fe}}{2} E_x \cos 2\varphi + \frac{a_{Ho}}{2} E_x (\cos 2\varphi + h^2 \cos 2\varphi_H) + F_{in}(\varphi) - \frac{\chi}{2} H^2 \sin^2(\varphi - \varphi_H). \quad (3)$$

Here $h = H/H_{ex}$ and ϵ_p is the dielectric permeability of the parphase. Using the relationship

$$D_x = -4\pi \partial \tilde{F} / \partial E_x,$$
¹⁴ we find the polarization

$$P_x = -0.5(a_{Fe} + a_{Ho}) \cos 2\varphi - 0, 5a_{Ho}h^2 \cos 2\varphi_H. \quad (4)$$

The effective dielectric permeability is defined from the relationship $\epsilon^{eff} = \partial D_x / \partial E_x$. These calculations are performed taking into account that the equilibrium value φ is an implicit function of the external variable fields. As noted in the Introduction, this is also a consequence of the existence of the electrical susceptibility of rotation. As a result, we have:

$$\frac{\epsilon^{eff} - \epsilon_p}{4\pi} = \frac{(\partial^2 \tilde{F} / \partial \varphi \partial E_x)^2}{\partial^2 \tilde{F} / \partial \varphi^2} = \frac{a^2 \sin^2 2\varphi}{r^2 - \chi H^2 \cos 2(\varphi - \varphi_H)}. \quad (5)$$

In (5), the designations are entered: $a = a_{Fe} + a_{Ho}$ and $r^2 = \partial^2 F_{in} / \partial \varphi^2$.

Any reasonable measurements of the parameters of magnetoelectric interaction are possible only in a single-domain sample, i.e. in the spin-flop phase. In this case $\varphi = \varphi_H + \pi/2$, and (5) is rewritten as

$$\frac{\delta \epsilon}{4\pi} \equiv \frac{\epsilon^{eff} - \epsilon_p}{4\pi} = \frac{a^2 \sin^2 2\varphi_H}{r^2(\varphi_H) - \chi H^2}. \quad (6)$$

It is clear that in the cases $\varphi_H = 0, \pi/2$ the recorded changes to ϵ_{xx}^{eff} are reflected in the general single-domain process and do not permit estimating the parameter of magnetoelectric association. As emphasized in Ref. 5, the optimal choice in that case is $\varphi_H = \pi/4$. Figure 2 visually illustrates these reasons, and it is specifically by them that we were guided in the representation of results in Fig. 1.

Figure 3 presents the magnetic-field dependences of ϵ at various temperatures and $\varphi_H = \pi/4$. In the limit of a large field, the change in ϵ represents a linear function of H^2 , by the slope of which, knowing the susceptibility χ , it is possible to determine the parameter of magnetoelectric coupling a . But since in this region of fields the spin-dependent response is already rather small, it is more convenient to introduce a new field function $y(H) = 1/(H_0^2 + H^2)$ ($\chi H_0^2 = r^2(\varphi_H)$) and to select an H_0 parameter that makes it possible to present change of ϵ in the form of a linear dependence on $y(H)$ throughout the interval of existence of the single-domain phase.⁶ An example of such a construction is given in the inset to Fig. 2.

Using reference data on the values of χ and $\epsilon_p = 20$,⁹ the development of the parameter of magnetoelectric coupling a with temperature (Fig. 4) is easily determined. From these data, in accordance with (4), the expected maximum value of polarization ($\sim 0.5a$) in a single-domain field ($T = 6$ K,

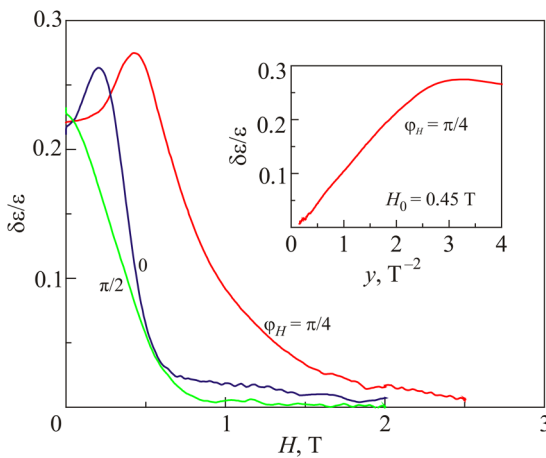


Fig. 2. Magnetic field dependences of relative changes of dielectric permeability for various orientation of the field in the base plane ($T = 6.5$ K). Inset: dielectric permeability as linearizing coordinates $y(H) = 1/(H_0^2 + H^2)$ (details in text).

$H = 0.5$ T) is $P_{\max} \sim 400\text{-}500 \mu\text{C}/\text{m}^2$. As measurements in Sm⁵ and Nd⁶ ferroborates have shown, the estimate P_{\max} that is analogous in the method obtained is underestimated by approximately a factor of two by comparison with static data, evidently as a consequence of frequency dispersion. However, in the case of Ho, static measurements of polarization provided values an order of magnitude smaller.⁹ One may assume that because of enantiomorphism the sample investigated in Ref. 9 had approximately an equal ratio of left and right modifications, which then resulted in almost complete compensation of the effect. At the same time, as noted above, the increase in dielectric permeability measured in Ref. 9 for $H = 0$ significantly exceeded our result. Since the change $\epsilon_{\text{eff}} \sim a^2$, enantiomorphism plays no role. It remains thus to assume that the samples studied in Ref. 9 and in this article differed essentially both in the domain structure, and in the value of the parameter r^2 . Note that extrapolation of the linear course of $\delta\epsilon/\epsilon_0$ in the region of small fields (inset in Fig. 2), which would correspond to measurements in an initially single-domain sample, also results in almost double increase in ϵ .

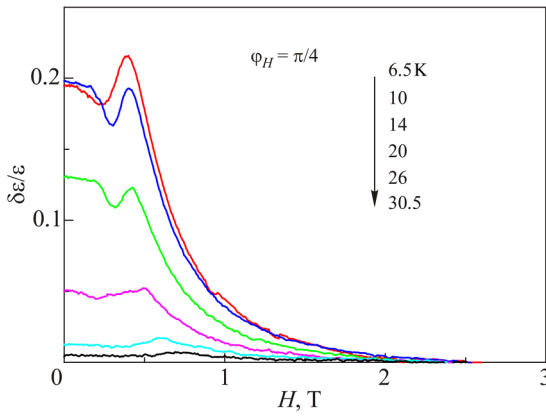


Fig. 3. Magnetic field dependences of relative changes of dielectric permeability for various temperatures. The maximum on each curve corresponds to the field of spin reorientation. (For $T = 6.5$ K, the dependence in Fig. 3 and the analogous one in Fig. 2 differ slightly because they were measured on different samples).

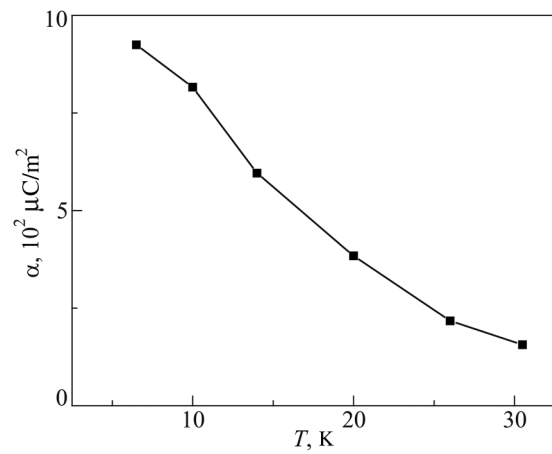


Fig. 4. Temperature dependence of the parameter of magnetoelectric coupling.

Magnetopiezoelectric effect

Figure 5 shows the development of the piezomodulus $e_{11}^{\text{eff}} \equiv e_{xxx}^{\text{eff}}$ in the antiferromagnetic phase for $H = 0$. Its comparison with the background dependence obtained by measurement in the stronger field indicates the nonmonotonic nature of the change of e_{11}^{eff} with temperature: the initial decrease in the piezomodulus is replaced by its rapid increase. A similar effect has been observed earlier in $\text{NdFe}_3(\text{BO}_3)_4$.⁶ Figure 6 shows the magnetic-field dependences of e_{11}^{eff} at various temperatures. As the field increases, the effective piezomodulus approaches its value in the paraphase. Therefore, in the low-temperature region, e_{11}^{eff} decreases as H increases and conversely increases for $T > 20$ K. The inset in Fig. 6 shows this increase in an expanded scale.

For a phenomenological description of magnetopiezoelectric effect (MPE) (3), it is necessary to add the thermodynamic potential by means of components that describe both the piezoeffect ($e_{11}E_xu_{xx}$, where e_{11} is the piezomodulus of the paraphase), and magnetoelastic interaction. This last is represented by components that are analogous to magnetoelectric ones, replacing E_x by deformation u_{xx} and the coefficients of magnetoelastic coupling a by the partial magnetoelastic coefficients b .^{5,6} The piezomodulus is calculated within the

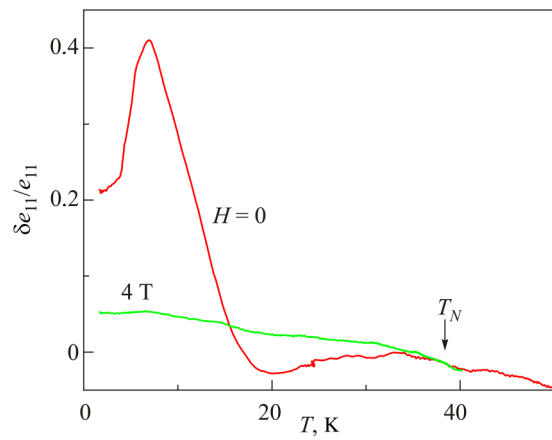


Fig. 5. Temperature dependence of relative changes of the piezomodulus ($H = 0$). The dependence for $H = 4$ T ($\varphi_H = 0$) is presented as the reference line, deviations from which indicate the change in direction of the piezomodulus in the magnetic-ordering phase.

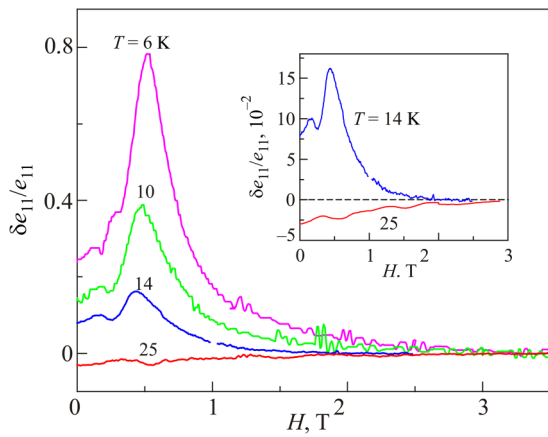


Fig. 6. Magnetic field dependences of relative changes of the piezomodulus for various temperatures. Inset: expanded scale for higher temperatures.

framework $e_{11}^{\text{eff}} = \partial\sigma_{xx}/\partial E_x = \partial^2 F / \partial E_x \partial u_{xx}$ (where σ_{xx} is in this case a real component of the tensor of the stresses). As a result, we derive:⁵

$$\delta e_{11} \equiv e_{11}^{\text{eff}} - e_{11} = -\frac{abs\sin^2 2\varphi}{r^2 - \chi H^2 \cos 2(\varphi - \varphi_H)}. \quad (7)$$

In (8), $b \equiv b_{\text{Fe}} + b_{\text{Ho}}$ is the parameter of magnetoelastic interaction.

Using the linearization procedure described above for $\varphi_H = \pi/4$, combining (6) and (7), and bringing in the values of the parameter a (Fig. 4) and e_{11} (Table 2), we obtain an estimate of the parameter b (Fig. 7). The nonmonotonic change of e_{11}^{eff} noted above is associated with the fact that the coefficient b changes sign, passing through zero at $T \sim 15-20$ K.

Neutron experiments¹⁷ have shown that in HoFe₃(BO₃)₄, as well as in NdFe₃(BO₃)₄, there is a helicoidal phase below 20 K. It is clear from general considerations that anisotropy in the base plane must be minimal for this to be available. Evidently, the chief contribution to this is brought by heterogeneities of magnetoelastic origin, the scale of which is defined by the same parameter b ,³ and consequently the zeroing of the latter also provides, in our opinion, the necessary conditions for the occurrence of a helicoid.

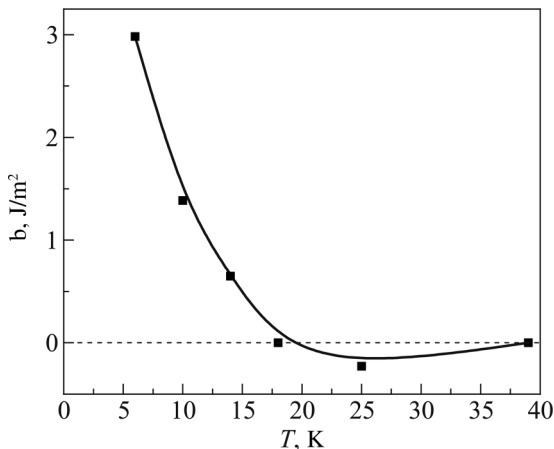


Fig. 7. Temperature dependence of the parameter of magnetoelastic association.

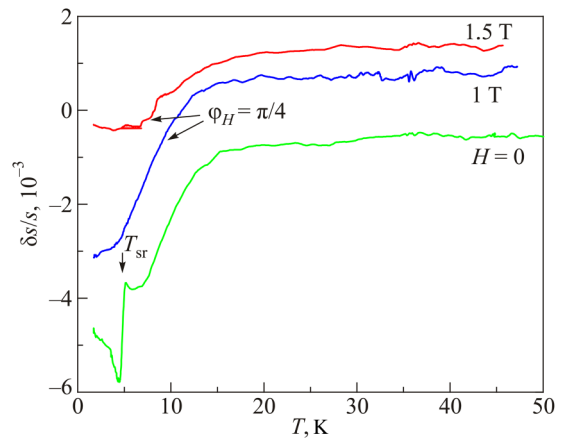


Fig. 8. Temperature changes of the velocity u_{xx} of the mode for various magnetic fields. In the paraphase, the velocity of sound does not depend on H , but for convenience of consideration the curves are displaced relative to each other.

Spin-dependent effects on sound velocity

Figure 8 illustrates the nature of the temperature changes of velocity of longitudinal sound extending along the x axis. At first, the velocity hardly changes below T_N , and a rapid fall begins below 20 K. Then, for $T_{sr} \approx 4.7$ K, there is observed a sharp decrease of velocity corresponding to a spontaneous spin-reorientation transition from the easy-plane to the easy-axis magnetic configuration.

We bring attention to the fact that the effects caused by the susceptibilities of rotation practically disappear upon transition to the easy-axis phase; both the dielectric permeability (Fig. 1) and the piezomodulus (Fig. 5) exceed slightly their values in the paraphase. At the same time the spin-dependent contribution to sound velocity even increases in this phase (Fig. 8, jump with reduction of velocity at $T_{sr}, H=0$) and remains significant while the system is in this state ($T \leq 5$ K, $H \leq 1$ T). In large fields, the spin reorientation into the easy-plane state that is stimulated by this field is completed, and the sound velocity approaches the value in the paraphase.

Figure 9 shows an example of the magnetic field dependences of velocity for various orientations of the field in the basic plane.

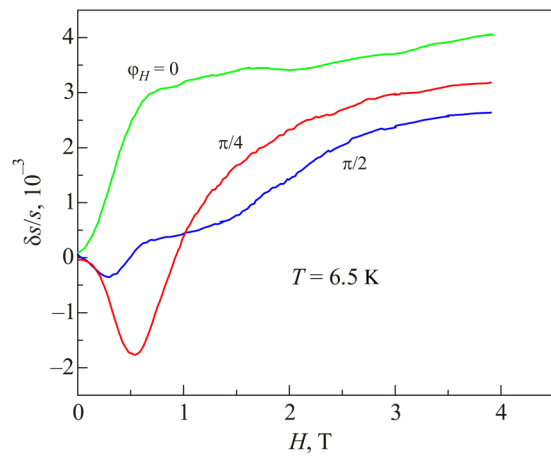


Fig. 9. Magnetic field dependences of relative changes of the velocity u_{xx} of the mode at various orientations of \mathbf{H} in the base plane.

For $\varphi_H = \pi/4$, the result is linearized by the same function $y(H)$, and for field direction along the coordinate axes the change is more complex. A characteristic property of the presented dependences is the fact that within a strong field the velocity depends on its orientation (Fig. 9). A similar effect was observed earlier in neodymium ferroborate⁶ and is associated with direct renormalization of the piezoelectric interaction in the spin-ordered phase. The corresponding contribution to \tilde{F} is described by the term $\tilde{e}_{11}E_x u_{xx} \cos 2\varphi$ by symmetry with reference to concrete deformation. This can be examined as the result of the decomposition of the parameter of magnetoelectric coupling a into a series by deformation.

Calculation of the spin-dependent effects in the moduli of elasticity is performed on the basis of the thermodynamic potential presented above, augmented with a component that corresponds to elastic energy. For a mode with shift u_x extending in the x_k direction, it is necessary to calculate the restoring force:

$$f_i = \frac{\partial \sigma_{ik}}{\partial x_k} = \frac{\partial^2 \tilde{F}}{\partial u_{ik} \partial x_k} = \frac{\partial^2 \tilde{F}}{\partial u_{ik} \partial E_k} \frac{\partial E_k}{\partial x_k} + \frac{\partial^2 \tilde{F}}{\partial u_{ik}^2} \frac{\partial u_{ik}}{\partial x_k}. \quad (8)$$

We define the derivative $\partial E_k / \partial x_k$ entering (8) from the equation of electroneutrality $\operatorname{div} \mathbf{D} = 0$:

$$\frac{\partial E_k}{\partial x_k} = \frac{\partial^2 \tilde{F} / \partial E_k \partial u_{ik}}{\partial^2 \tilde{F} / \partial E_k^2} \frac{\partial u_{ik}}{\partial x_k}.$$

Substituting this expression into (9), we obtain:

$$f_i = \left\{ \frac{4\pi(e_{ik}^{\text{eff}})^2}{\epsilon^{\text{eff}}} + \frac{\partial^2 \tilde{F}}{\partial u_{ik}^2} \right\} \frac{\partial u_{ik}}{\partial x_k}. \quad (9)$$

The expression in curly brackets in (9) also represents the effective modulus of elasticity C_{ik} . In the paraphase, with deformation u_{xx} this results in the well-known renormalization of sound velocity due to the piezoeffect:¹⁴ $\rho s^2 = C_{11} + 4\pi e_{11}^2 / \epsilon$. In the magnetic-ordered state this is supplemented with a contribution from magnetoelastic interaction. Within a strong field, all renormalizations associated with rotary susceptibility are set to zero, and there is only a contribution from \tilde{e}_{11} . For $\tilde{e}_{11}/e_{11} \ll 1$, the velocities of sound for $\varphi_H = 0, \pi/2$ differ by the value

$$\frac{\delta s}{s} = \frac{8\pi e_{11} \tilde{e}_{11}}{\epsilon_p \rho s^2}. \quad (10)$$

It follows from the data presented in Fig. 9 that at 6.5 K, $\tilde{e}_{11}/e_{11} \approx 1, 7\%$, which exceeds by a factor of two the similar estimate for $\text{NdFe}_3(\text{BO}_3)_4$.⁵

A neutron experiment¹⁵ observed that in the easy-plane phase with $H=0$, the vector of antiferromagnetism exits the base plane by a small angle. Generally speaking, such an effect is characteristic for trigonal and hexagonal antiferromagnets, and is associated with the very weak basic anisotropy of these objects (see Ref. 18).

In the absence of external perturbations, the situation is described by the addition to the thermodynamic potential of the invariants associated with the z -components of the vector of antiferromagnetism \mathbf{L} :

$$\tilde{F}(l_z) = \dots \frac{\beta}{2} l_z^2 - \gamma l_z \sin 3\varphi. \quad (11)$$

In (11), l_z is the directing cosine of the vector \mathbf{L} in relation to the z axis. The first component ($\beta > 0$) restrains the magnetic system from transition to the easy-axis phase, and the second represents an addition to the energy at an exit of spins from the base plane. Since spontaneous polarization \mathbf{P} appears in the compounds under study below T_N , one should add to the energy the component $P_z l_z \cos 3\varphi$, but such added complexity does not introduce changes in principle. Minimization of (11) determines that $l_z = \gamma/\beta \sin 3\varphi \ll 1$. In the homogeneous state for $H=0$, the state with $l_z \neq 0$ is achieved when certain restrictions on the parameters of easy-plane anisotropy are satisfied,¹⁸ but the effect always exists in the helicoidal phase. This reduces to modulation of \mathbf{L} with a variable-sign exit from the base plane.

In a single-domain magnetic field, the angle φ is specified ($\varphi = \varphi_H + \pi/2$), and $l_z \neq 0$ almost always, and so therefore the question reduces only to the effect of the size. Measurements of magnetic field changes of sound velocity make it possible to be convinced of the possibility of detecting it.

We presume at first that $l_z = 0$ and we will examine the change of velocity of the C_{44} mode extending along the z axis. For this purpose, it is necessary to add to the thermodynamic potential the fragments of invariant components that correspond to the magnetoelectric and magnetoelastic interaction that are of current interest for the geometry discussed with this mode: $\tilde{F}_1 = \dots a_1 E_z \sin 6\varphi + b_1 u_{xz} \sin 2\varphi \dots$. For the calculations in (9), there will necessarily be multipliers $\partial^2 \tilde{F}_1 / \partial E \partial \varphi$ and $\partial^2 \tilde{F}_1 / \partial u \partial \varphi$. After selecting $\varphi_H = \pi/4$, we see that the contribution to sound velocity in this geometry is set to zero, i.e., one should not expect characteristic dependences proportional to H^2 .

Now let $l_z \neq 0$. We add to \tilde{F} in addition to \tilde{F}_1 the corresponding components: $\tilde{F} = \dots a_2 E_z l_z \cos 3\varphi + b_2 u_{xz} l_z \cos \varphi \dots$. In substituting the equilibrium value $l_z \sim \sin 3\varphi$, the component $b_2 \gamma/\beta \sin 4\varphi$ appears in \tilde{F}_2 . In the same geometry ($\varphi_H = \pi/4$), the calculation in (9) has a nonzero result due to this component. Returning to the velocity C_{44} of the mode, we arrive at the relationship

$$\frac{\delta s}{s} = - \frac{2 \left(b_2 \frac{\gamma}{\beta} \right)^2}{\chi(H_0^2 + H^2) \rho s^2}. \quad (12)$$

It follows from (12) that the sound velocity must increase as the field increases. The scale of changes is defined by the combination of constants $b_2 \gamma/\beta$. Figure 10 shows the results of measurements for the corresponding geometry in $\text{HoFe}_3(\text{BO}_3)_4$.

The characteristic increase of velocity in the fields that exceed the magnetic spin-flop field H_{SF} is observed at both low and high temperatures. However, in the region of intermediate temperatures (10–18 K), the effect is practically absent. We presume that the parameter $b_2(T)$, as well as $b(T)$, passes through zero value in this temperature region. Nonmonotonic change of the parameter γ is possible as well. As also earlier, in the region of existence of the effect, the field dependences are linearized by the function $y(H)$. An example of such construction is given in the inset to Fig. 10. The parameter $b_2 \gamma/\beta \approx 4.6 \cdot 10^6 \text{ J/m}^3$ is defined at 6 K from the slope of the straight line. If we assume that the

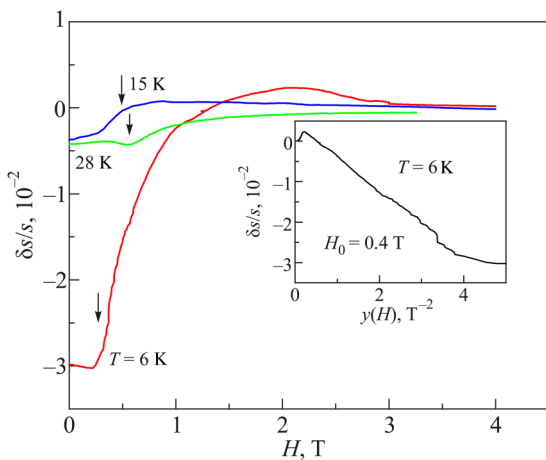


Fig. 10. Magnetic field dependences of the relative changes of the velocity C_{44} of the mode in $\text{HoFe}_3(\text{BO}_3)_4$ for various temperatures ($\phi_H = \pi/4$). The spin-flop field for each dependence is specified by an arrow. Inset: velocity as a function of the linearizing function $y(H) = 1/(H_0^2 + H^2)$.

coefficients b_2 and b are of the same order of magnitude ($3 \cdot 10^7 \text{ J/m}^3$, see Fig. 7), then we obtain at this temperature the estimate $\gamma/\beta \sim 0.1\text{--}0.2$, i.e., the vector of antiferromagnetism is inclined from the base plane at an angle $\sim 5^\circ$.

It follows from the above-mentioned that similar dependences must also be observed in other ferroborates that are ordered in the easy-plane configuration. Measurements in the same geometry of the velocity C_{44} of the mode in samarium ferroborate (Fig. 11) were performed in order to verify this statement.

From the given dependences, one may conclude that, unlike $\text{HoFe}_3(\text{BO}_3)_4$, the parameter $b_2(T)$ in $\text{SmFe}_3(\text{BO}_3)_4$ changes monotonically, as also the parameter $b(T)$.⁵ At 6 K, the combination $b_2 \gamma/\beta \approx 2 \cdot 10^6 \text{ J/m}^3$. With the same assumption for the order of magnitude $b_2 \sim b$, ($\sim 1.8 \cdot 10^7 \text{ J/m}^{35}$), we find $\gamma/\beta \sim 0.1$.

Let us say a few words about the velocity of the u_{xx} mode in the easy-axis phase (Fig. 8). The appearance of the component $-vE_x u_{xx} l_z/2$, which is actually also a renormalization of the piezoelectric interaction under the influence of magnetic ordering, is possible by symmetry in the decomposition of the thermodynamic potential in this case. Calculating (9) in accordance with the result of Fig. 8, we obtain the estimate $v/e_{11} \sim 0.1$ for $l_z = 1$.

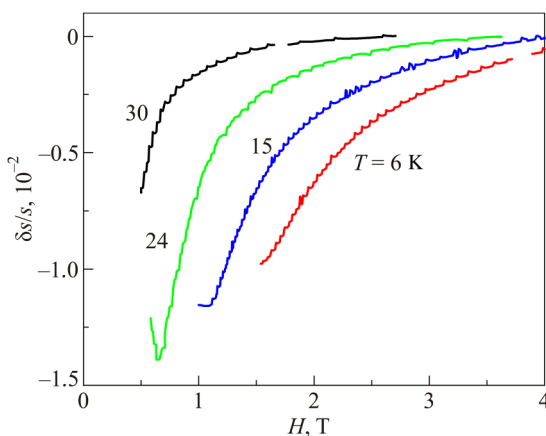


Fig. 11. Magnetic field dependences of relative changes of the velocity C_{44} of the mode in $\text{SmFe}_3(\text{BO}_3)_4$ for various temperatures ($\phi_H = \pi/4$).

Conclusion

The main components of the tensor of the moduli of elasticity are measured in $\text{HoFe}_3(\text{BO}_3)_4$ monocrystals. The value of the piezomodulus found in the paraphase $e_{xxx} = 1.44 \text{ C/m}^2$ makes it possible to relate this association, as well as the ferroborates of samarium and neodymium, to the class of strong piezoelectric materials. The constants of magnetoelectric and magnetoelastic interactions that exceed the analogous values for ferroborates of samarium and neodymium are measured in the antiferromagnetic phase. One may expect that the value of electric polarization in the studied connection with a predominance of right- or left-handed isomers must reach the values of $\sim 1000 \mu\text{C/m}^2$. The constant of magnetoelastic interaction at $T \sim 15\text{--}20 \text{ K}$ changes sign, leading it appears to the appearance of a helicoidal type of magnetic ordering. The spin-dependent effects in the behavior of the velocity of sound were studied. Experiments were performed, confirming the exit of the vector of antiferromagnetism from the base plane at an angle $\sim 5^\circ$ in the crystals in the spin-flop state.

^{a)}Email: fil@ilt.kharkov.ua

- ¹A. M. Kadomtseva, Yu. F. Popov, G. P. Vorob'ev, A. P. Pyatakov, S. S. Krotov, K. I. Kamilov, V. Yu. Ivanov, A. A. Mukhin, A. K. Zvezdin, A. M. Kuz'menko, L. N. Bezmaternykh, I. A. Gudim, and V. L. Temerov, FNT, **36**, 640 (2010) [Low Temp. Phys., **36**, 511 (2010)].
- ²I. A. Gudim, V. L. Temerov, E. V. Eremin, N. V. Volkov, and M. S. Molokeev, *Racemism and Macroscopic Magnetolectric Effects in Trigonal Rare Earth Oxyborates*, Theses of Reports of the V Baikal International Conference "Magnetic Materials. New Technologies" [in Russian], Irkutsk (2012), 82 pp.
- ³A. A. Mukhin, G. P. Vorob'ev, V. Yu. Ivanov, A. M. Kadomtseva, A. S. Narizhny, A. M. Kuz'menko, Yu. F. Popov, L. N. Bezmaternykh, and I. A. Gudim, Pis'ma v ZhETF, **93**, 305 (2011) [JETP Lett., **93**, 275 (2011)].
- ⁴A. K. Zvezdin, G. P. Vorob'ev, A. M. Kadomtseva, Yu. F. Popov, A. P. Pyatakov, L. N. Bezmaternykh, A. V. Kuvardin, and E. A. Popova, Pis'ma v ZhETF, **83**, 600 (2006) [JETP Lett., **83**, 509 (2006)].
- ⁵T. N. Gaidamak, I. A. Gudim, I. V. Bilych, N. G. Burma, K. R. Zhekov, and V. D. Fil, Phys. Rev. B, **92**, 214428 (2015).
- ⁶I. V. Bilych, K. R. Zhekov, T. N. Gaidamak, I. A. Gudim, G. A. Zvyagina, and V. D. Fil', FNT, **42**, 1419 (2016) [Low Temp. Phys., **42**, 1112 (2016)].
- ⁷L. S. Kolodyazhnaya, G. A. Zvyagina, I. A. Gudim, I. V. Bilych, N. G. Burma, K. R. Zhekov, and V. D. Fil', FNT, **43**, 1151 (2017) [Low Temp. Phys., **43**, 924 (2017)].
- ⁸V. D. Fil, M. P. Kolodyazhnaya, G. A. Zvyagina, I. V. Bilych, and K. R. Zhekov, Phys. Rev. B, **96**, 180407 (R) (2017).
- ⁹R. P. Chaudhury, F. Yen, B. Lorenz, Y. Y. Sun, L. N. Bezmaternykh, V. L. Temerov, and C. W. Chu, Phys. Rev. B, **80**, 104424 (2009).
- ¹⁰T. N. Gaidamak, I. A. Gudim, G. A. Zvyagina, I. V. Bilych, N. G. Burma, K. R. Zhekov, and V. D. Fil', FNT, **41**, 792 (2015) [Low Temp. Phys., **41**, 614 (2015)].
- ¹¹V. I. Zinenko, M. S. Pavlovskii, A. S. Krylov, I. A. Gudim, and E. V. Eremin, ZhETF, **144**, 1174 (2013).
- ¹²L. N. Bezmaternykh, V. L. Temerov, I. A. Gudim, and N. A. Stolbovaya, Crystallogr. Rep., **50**, S97 (2005).
- ¹³E. A. Masalitin, V. D. Fil', K. R. Zhekov, A. N. Zholobenko, T. V. Ignatova, and S. I. Lee, FNT, **29**, 93 (2003) [Low Temp. Phys., **29**, 72 (2003)].
- ¹⁴L. D. Landau and E. M. Lifshitz, *Electrodynamics of Continuous Media* [in Russian], Nauka, Moscow (1982).
- ¹⁵C. Ritter, A. Vorotynov, A. Pankrats, G. Petrakovskii, V. Temerov, I. Gudim, and R. Szymczak, J. Phys. Cond. Matter, **20**, 365209 (2008).
- ¹⁶A. A. Demidov and D. V. Volkov, FTT, **53**, 926 (2011).
- ¹⁷D. K. Shukla, S. Francoual, A. Skaugen, M. V. Zimmermann, H. C. Walker, L. N. Bezmaternykh, I. A. Gudim, V. L. Temerov, and J. Strempfer, Phys. Rev. B, **86**, 224421 (2012).
- ¹⁸E. A. Turov, A. V. Kolchanov, V. V. Men'shenin, I. F. Mirsaev, and V. V. Nikolaev, *Symmetry and Physical Properties of Antiferromagnets*, Fizmatgiz, Moscow (2004) [in Russian].